

Sensitivity Tests of a Two-layer Hydrodynamic Model in the Gulf of Finland with Different Atmospheric Forcings

K. Myrberg

Finnish Institute of Marine Research, P.O.Box 33, FIN-00931, Helsinki, Finland

(Received: April 1996; Accepted: January 1997)

Abstract

*A two-dimensional, two-layer baroclinic prognostic hydrodynamic model has been developed and compared with measurements of surface salinity and temperature, the thickness of the upper mixed layer and water level height. The model's ability to reproduce the main hydrographic features of the Gulf of Finland is tested. Special attention is paid to the role of atmospheric forcing. In the first simulation the atmospheric forcing derived from the observations of a single weather station (Kalbådagrund) was used. The results of this simulation were compared with the results of model runs, for which the atmospheric input was taken from the HIRLAM meteorological model. The accuracy of the results improved when the HIRLAM input was used. However, even the version of the HIRLAM model used, which had a horizontal resolution of 55*55 kilometres, could not accurately enough describe the complicated structure of the atmospheric wind and temperature fields over the narrow Gulf (width ca. 40-150 kilometres).*

Key words: two-layer model, sensitivity test, atmospheric forcing

1. Introduction

The Gulf of Finland (**GOF**) is an estuarine basin in the north-eastern Baltic Sea where marine hydrophysical features from small-scale vortices up to a large-scale circulation exist. It is a complicated hydrographic region with a saline water input from the Baltic Proper and with a large fresh water input from rivers. Because of the large horizontal salinity gradients, both density and wind-driven currents play a dominant role in the circulation. The complicated bottom topography favours the formation of mesoscale circulation patterns, fronts and eddies. The hydrography of the GOF is also characterized by seasonal variations of stratification. The oblong shape of the GOF leads to complicated atmospheric patterns in terms of a horizontally-inhomogeneous distribution of surface roughness and thermal forcing. On the other hand, the geographically limited size makes it possible to cover the area with oceanographic observations having a dense spatial and temporal resolution.

During recent decades several two-dimensional and three-dimensional numerical prognostic models have been developed. A review of the Baltic Sea models has been given by *Svansson* (1976) and by *Omstedt* (1989). Both types of models have been applied for determining various aspects of flow patterns, water level variability, temperature and salinity distributions. The first two-dimensional model was developed by *Hansen* (1956) using linearized barotropic equations, in order to simulate the severe flood which took place in the Netherlands in 1953. *Welander* (1966, 1968) has developed several versions of two-dimensional models. *Welander* (1968) used the linearized two-dimensional model for studies of the Gulf Stream. *O'Brien* (1967), *O'Brien* and *Hurlburt* (1972) used their nonlinear two-layer, two-dimensional flow model for studies of upwellings. Other important two-dimensional approaches have been introduced e.g. by *Laevastu* (1973) and by *Heaps* (1985). For Baltic Sea studies, several two-dimensional models have been developed. *Kowalik* (1969, 1972) used a barotropic two-dimensional model. Later on, applications relating to the importance of the water exchange between the Baltic Sea and the North Sea were studied (*Kowalik* and *Staskiewicz*, 1976; *Chilika*, 1984; *Chilika* and *Kowalik*, 1984). Applications of two-dimensional barotropic models have also been used e.g. by *Tamsalu* (1967) for Tallinn Bay, and by *Voltizinger* and *Simuni* (1963) and by *Laska* (1966) for storm-surge problems in several parts of the Baltic Sea. Several approaches using two-dimensional models have been made in Finland too. *Uusitalo* (1960) employed a barotropic model version to investigate currents in the Gulf of Bothnia. *Sarkkula* and *Virtanen* (1978) applied a two-dimensional model to the Bothnian Bay around the Kokemäenjoki river for water management purposes. *Jokinen* (1977) used a barotropic model for his studies of the Gulf of Bothnia, while *Häkkinen* (1980) applied such a model to the whole Baltic Sea, including the Danish Straits, to calculate water level heights. *Myrberg* (1992) used a two-dimensional, two-layer linear model for studies of climatological circulation in the Gulf of Finland and the Gulf of Bothnia.

During the 1970's three-dimensional model development started actively in many research institutes around the world. The first such model was developed by *Bryan* (1969), whose model was used for studies of the World Ocean. The model has later been modified many times (*Killworth* et al., 1991) and the latest modified version is in common use. *Simons* (1974) developed a three-dimensional model for the Great Lakes in Canada. *Blumberg* (1977), *Blumberg* and *Mellor* (1987) have developed a three-dimensional model, in which a sigma-coordinate system is used in the vertical direction. This model is also widely used in different institutes. *Davies* (1980) has used his models for many different areas e.g. for water bodies around the U.K.. Among the numerous three-dimensional models, the following approaches are also worth mentioning. *Müller-Navarra* (1983) has carried out simulations for the Baltic Sea and North Sea areas; operational modelling is also an ongoing activity. *Backhaus* (1985) has developed a model for the North Sea, but applications to other sea-areas have been made too. Recently, *Oberhuber* (1993) has constructed an isopycnal ocean circulation model. In

the Baltic Sea area, many of the abovementioned three-dimensional models have been used. *Simons* (1976, 1978) applied his model to the Baltic Sea and studied the role of topography, stratification and boundary conditions in the wind-driven circulation. *Kielmann* (1981) continued the studies of currents and water-level heights using *Simons'* model. *Funkquist* and *Gidhagen* (1984) have applied *Kielmann's* model version. *Krauss and Brügge* (1991), *Elken* (1994) and *Lehmann* (1995) have applied the Bryan-Cox-Semtner-Killworth free-surface model version (*Killworth*, 1991) for studying various aspects of the physics of the Baltic Sea. *Klevanny* (1994) has developed a modelling system of two-and three-dimensional models for studying various water bodies: rivers, lakes and seas (including the Baltic Sea). *Andrejev* and *Sokolov* (1992) and *Andrejev et al.*, (1992) have developed a three-dimensional model, which has been used e.g. for dispersion studies in the Gulf of Finland. In Finland a three-dimensional model has been developed by *Koponen* (1984). The model has been used for various types of case studies and for operational use (*Koponen et. al.*, 1994). *Tamsalu* (1996) has recently developed a three-dimensional isopycnal model for the Baltic Sea, the two-dimensional version of which is studied in this paper.

The reader further interested in modelling is referred to e.g. the following textbooks: *Nihoul* (1982), *O'Brien* (1986), *Nihoul and Jamart* (1987) and *Kowalik and Murty* (1993). All the abovementioned textbooks include both the theoretical and the practical aspects of oceanographic models of various kinds.

The three-dimensional models are those most used today and also naturally the most complete. However, a hierarchy of models of different orders of complexity is still needed to realize the advantages and circumvent the limitations of the various types of models (*Davies*, 1994). A parallel two-dimensional and three-dimensional coupled hydrodynamic-ecosystem modelling study is an ongoing part of Finnish-Estonian cooperation (*Tamsalu and Myrberg*, 1995; *Tamsalu and Ennet*, 1995; *Tamsalu*, 1996).

In this study a two-dimensional, two-layer baroclinic prognostic model with fully nonlinear hydrothermodynamical equations is used. A look is given at the main equations of the model. According to *Nihoul* (1994), the right procedure for deriving a realistic two-dimensional model from a three-dimensional one is by integration of the equations over depth. The derivation of the two-dimensional equations from the three-dimensional ones is shown in detail. The results of the model are compared with CTD-measurements (from 1992) of surface salinity and temperature and of thickness of the upper mixed layer as well as with observations of water level height. The analysis of the model results is focused on August 1992. This is because at that time there were enough CTD-data available for the western GOF-northern Baltic Proper area, making it possible to determine accurate boundary conditions for the model's open boundary in the west. The model tests were carried out for the upper mixed layer of the sea. Comparison of the model results with currents has not been carried out, because the two-dimensional model gives vertically-integrated currents in both layers, while the long-term eulerian

current measurements give currents at 2-3 prescribed levels, from which the vertical integration of current is difficult to carry out.

The main idea of the paper is the testing of the model's response to atmospheric forcings of various kinds. Firstly, measured values of atmospheric temperature, wind speed and direction, clouds and humidity from a single weather station over the open part of the GOF (Kalbådagrund) are used as atmospheric input to the model for the whole GOF. Secondly, the meteorological input is taken from the HIRLAM (High Resolution Limited Area Modelling; *Machenhauer, 1988, Gustafsson, 1991*) atmospheric model. On the other hand, the paper tries to demonstrate to what extent the two-dimensional model can produce the main characteristics of the hydrodynamic variables in the upper mixed layer of the sea.

2. *Hydrodynamic baroclinic prognostic two-layer model*

The present two-dimensional model is a modified version of the model described by *Tamsalu and Myrberg (1995)*. In that older version the equations were derived in order to solve the marine system variables in the upper layer and for the vertically-integrated means of the variables. In the new version the equations are derived for both the upper and bottom layers. A new feature is an evolution equation for the prediction of water level heights. The corresponding model results are compared with observations in this paper. The atmospheric input in the older version was taken from a single weather station, whereas in the present version the effects of the spatial variability of atmospheric forcing is investigated too. This study tries to present a view of the physical processes occurring on time scales ranging from some hours to several days, whereas in the study by *Tamsalu and Myrberg (1995)* mostly the monthly mean values for marine system variables were investigated.

2.1 *Derivation of the two-dimensional model equations from the three-dimensional structure*

In the following, the derivation of the two-dimensional equations is shown starting from the three-dimensional equations presented by *Tamsalu (1996)*.

In the sea there are principally two layers: the upper mixed layer and the lower stratified layer. In the upper mixed layer of the sea the microturbulence (vertical turbulence) is caused mainly by breaking of the wind waves and by instability of the wind drift. Experimental investigations have shown (see for example *Miropolsky, 1981*) that outside the boundary layers turbulence is weak and intermittent in character. Taking into account the different hydrophysics in the different layers, the equations can be written in the coordinate system $\sigma_i = (z_i - h_i) / D_i$, where $i=1,2$; $i=1$ represents the upper layer, $i=2$ the lower stratified layer, $D_1 = (h_2 - h_1) = (h_2 - Z)$ is the mixed layer thickness; $h_1 = Z$ is the sea level oscillation; $D_2 = (h_3 - h_2) = (H - h_2)$ is the thickness

of the lower stratified layer; h_2 is the interface between the upper and lower layer, $h_3 = H$ is the sea depth. A detailed analysis of the 3D model equations as well as of the numerical analysis is given by *Tamsalu* (1996).

According to the system described above, the equations of motion can be written as follows:

$$\frac{\partial c_i}{\partial t} + (L_1 + L_2)c_i = F_i \quad (1)$$

The continuity equation is written:

$$\frac{\partial u_i D_i}{\partial x} + \frac{\partial v_i D_i}{\partial y} + \frac{\partial \omega_i}{\partial \sigma_i} = 0 \quad (2)$$

The equation for the vertical variations takes the form:

$$\frac{1}{\rho_0} \frac{\partial p_i}{\partial \sigma_i} = g D_i \frac{(\rho_i - \rho_0)}{\rho_0} = b_i \quad (3)$$

$$b_i = \alpha(T_i - T_0)^2 - \beta(S_i - S_0) \quad (4)$$

where:

$$\omega_i = w_i - u_i \frac{\partial \delta_i}{\partial x} - v_i \frac{\partial \delta_i}{\partial y}; \quad \delta_i = h_i + \sigma_i D_i$$

$$c_i = \left\{ \begin{array}{c} u_i \\ v_i \\ T_i \\ S_i \end{array} \right\}$$

$$F_i = \left\{ \begin{array}{c} -\frac{1}{\rho_0} \frac{\partial p_i}{\partial y} - b_i \frac{\partial \delta_i}{\partial y} - f v_i \\ -\frac{1}{\rho_0} \frac{\partial p_i}{\partial x} - b_i \frac{\partial \delta_i}{\partial x} + f u_i \\ \frac{1}{c_p \rho_0 D_i} \frac{\partial I}{\partial \sigma_i} \\ 0 \end{array} \right\}$$

$$L_1 c_i = u_i \frac{\partial c_i}{\partial x} + v_i \frac{\partial c_i}{\partial y} + \frac{1}{D_i} \left(\frac{\partial \overline{u_i c_i D_i}}{\partial x} + \frac{\partial \overline{v_i c_i D_i}}{\partial y} \right)$$

$$L_2 c_i = \frac{1}{D_i} (\omega_i - \frac{\partial \delta_i}{\partial t}) \frac{\partial c_i}{\partial \sigma_i} + \frac{1}{D_i} \frac{\partial \overline{\omega_i c_i}}{\partial \sigma_i}$$

Here:

x is directed to the east, y is directed to the north and z is directed downwards, $u_i, v_i, w_i, \omega_i, c_i$ represent averaged values, $u'_i, v'_i, w'_i, \omega'_i, c'_i$ represent turbulent fluctuations, U_i is the velocity vector with components u_i, v_i and w_i , T_i is the temperature, T_0 is a mean temperature, S_i is the salinity, S_0 is a mean salinity, p_i is the pressure, ρ_i is the density, ρ_0 is the mean density; b_i is the buoyancy, g is the acceleration due to gravity; f is the Coriolis parameter, I is the solar radiation; c_p is the specific heat of water, α is the coefficient of thermal expansion, β is an expansion coefficient for salinity (for details, see *Zilitinkevich, 1991*).

2.1.1 Parameterization of turbulent fluxes

The turbulent fluxes are parameterized using traditional turbulent coefficients.

$$\overline{u'_i c'_i} D_i = -\mu D_i \frac{\partial c_i}{\partial x}; \overline{v'_i c'_i} D_i = -\mu D_i \frac{\partial c_i}{\partial y}; \overline{\omega'_i c'_i} D_i = -\nu \frac{\partial c_i}{\partial \sigma_i} \quad (5)$$

Here:

μ is the coefficient of macroturbulence, $\nu(Ri)$ is the coefficient of microturbulence, Ri is the Richardson number, $\overline{u'_i c'_i}$, $\overline{v'_i c'_i}$, $\overline{\omega'_i c'_i}$ are ensemble averages.

2.1.2 Boundary conditions

At sea level, where $\sigma_1 = 0$

$$\overline{u'_1 \omega'_1} = -\tau_{xz}^0; \overline{v'_1 \omega'_1} = -\tau_{yz}^0; \overline{T'_1 \omega'_1} = -q_T^0; \overline{S'_1 \omega'_1} = -q_S^0; \omega_1 = \frac{\partial Z_1}{\partial t} \quad (6)$$

$\tau_{xz}^0, \tau_{yz}^0, q_T^0, q_S^0$ will be calculated using atmospheric data (see, e.g. *Niiler and Kraus, 1977*).

At the bottom of the sea, where $\sigma_2 = 1$

$$\overline{u'_2 \omega'_2} = ru_2; \overline{v'_2 \omega'_2} = rv_2; \overline{T'_2 \omega'_2} = 0; \overline{S'_2 \omega'_2} = 0; \omega_2 = 0 \quad (7)$$

The bottom friction is parameterized as follows: $r = 1.510^{-3} \sqrt{u_2^2 + v_2^2}$.

In the coastal area we have:

$$u_i = v_i = 0; \frac{\partial T_i}{\partial n} = \frac{\partial S_i}{\partial n} = 0 \quad (8)$$

At the open boundary we have:

$$\frac{\partial u_i}{\partial n} = \frac{\partial v_i}{\partial n} = \frac{\partial T_i}{\partial n} = 0; S_i = \Gamma \quad (9)$$

where n is normal to the coastline and Γ is experimental data for salinity at the model's boundary.

2.1.3 The two-layer structure

In the upper mixed layer the hydrodynamic fields can be written as follows:

$$U_1 = U_1(t, x, y, \sigma_1); T_1 = T_1(t, x, y); S_1 = S_1(t, x, y) \quad (10)$$

Integrating equation (1) over the mixed layer, using (10), we obtain:

$$\frac{\partial \bar{c}_1}{\partial t} + \bar{L}_1 \bar{c}_1 = \bar{F}_1 \quad (11)$$

where:

$$\bar{c}_1 = \int_0^1 \left\{ \begin{array}{c} u_1 \\ v_1 \\ T_1 \\ S_1 \end{array} \right\} d\sigma_1$$

$$\bar{L}_1 \bar{c}_1 = \bar{u}_1 \frac{\partial \bar{c}_1}{\partial x} + \bar{v}_1 \frac{\partial \bar{c}_1}{\partial y} - \frac{1}{D_1} \left(\frac{\partial}{\partial x} \mu D_1 \frac{\partial \bar{c}_1}{\partial x} + \frac{\partial}{\partial y} \mu D_1 \frac{\partial \bar{c}_1}{\partial y} \right)$$

$$\bar{F}_1 = \left\{ \begin{array}{l} -\pi_{x1} - f\bar{v}_1 + \tau_{x1} / D_1 \\ -\pi_{y1} - f\bar{u}_1 + \tau_{y1} / D_1 \\ \frac{\alpha_1}{c_p \rho_0} I_0 (1 - e^{-\gamma h}) + q_{T1} / D_1 \\ q_{S1} / D_1 \end{array} \right\}$$

where:

$$\pi_{x1} = g \frac{\partial Z}{\partial x} + \frac{1}{2} \frac{\partial}{\partial x} (D_1 \bar{b}_1)$$

$$\pi_{y1} = g \frac{\partial Z}{\partial y} + \frac{1}{2} \frac{\partial}{\partial y} (D_1 \bar{b}_1)$$

$$\tau_{x1} = \tau_x^0 - \tau_x^h ; \quad \tau_{y1} = \tau_y^0 - \tau_y^h$$

$$q_{T1} = q_T^0 - q_T^h ; \quad q_{S1} = q_S^0 - q_S^h$$

$I = I_0 e^{-\gamma z} - I_0$ is the solar radiation at the sea-surface, γ is the coefficient of attenuation of solar radiation.

In the lower layer the hydrodynamic fields can be determined as follows:

$$U_2 = U_2(t, x, y, \sigma_2); \quad T_2 = T_2(t, x, y, \sigma_2); \quad S_2 = S_2(t, x, y, \sigma_2) \quad (12)$$

Integrating equation (1) over the lower layer using (12) we get:

$$\frac{\partial \bar{c}_2}{\partial t} + L_2 \bar{c}_2 = \bar{F}_2 \quad (13)$$

where:

$$\bar{c}_2 = \int_0^1 \left\{ \begin{array}{c} u_2 \\ v_2 \\ T_2 \\ S_2 \end{array} \right\} d\sigma_2$$

$$\bar{L}_2 \bar{c}_2 = \bar{u}_2 \frac{\partial \bar{c}_2}{\partial x} + \bar{v}_2 \frac{\partial \bar{c}_2}{\partial y} - \frac{1}{D_2} \left(\frac{\partial}{\partial x} \mu D_2 \frac{\partial \bar{c}_2}{\partial x} + \frac{\partial}{\partial y} \mu D_2 \frac{\partial \bar{c}_2}{\partial y} \right)$$

$$\bar{F}_2 = \left\{ \begin{array}{l} -\pi_{x2} - f\bar{v}_2 + \tau_{x2} / D_2 \\ -\pi_{y2} + f\bar{u}_2 + \tau_{y2} / D_2 \\ q_T^h / D_2 \\ q_S^h / D_2 \end{array} \right\}$$

$$\pi_{x2} = g \frac{\partial Z}{\partial x} + \frac{(D_1 + H)}{2} \frac{\partial \bar{b}_1}{\partial x} + \bar{b}_1 \frac{\partial D_1}{\partial x} + \bar{b}_2 \frac{\partial H}{\partial x} + c_0 D_2 \frac{\partial}{\partial x} (\bar{b}_2 - \bar{b}_1)$$

$$\pi_{y_2} = g \frac{\partial Z}{\partial y} + \frac{(D_1 + H)}{2} \frac{\partial \bar{b}_1}{\partial y} + \bar{b}_1 \frac{\partial D_1}{\partial y} + \bar{b}_2 \frac{\partial H}{\partial y} + c_0 D_2 \frac{\partial}{\partial y} (\bar{b}_2 - \bar{b}_1)$$

Here we use the relation:

$$2 \int_0^1 \int_0^{\sigma_2} b_2 d\sigma_2 d\sigma_2 - \bar{b}_1 = 2c_0 (\bar{b}_2 - \bar{b}_1)$$

$$c_0 = \text{const} \cong 1/3$$

$$\tau_{x_2} = \tau_x^h - r\bar{u}_2 ; \quad \tau_{y_2} = \tau_y^h - r\bar{v}_2$$

$$\tau_x^h = (\bar{u}_2 - \bar{u}_1)\Lambda^h ; \quad \tau_y^h = (\bar{v}_2 - \bar{v}_1)\Lambda^h$$

$$q_T^h = (\bar{T}_2 - \bar{T}_1)\Lambda^h ; \quad q_S^h = (\bar{S}_2 - \bar{S}_1)\Lambda^h$$

$$\Lambda^h = \frac{\partial D_1}{\partial t} \quad \text{if } \frac{\partial D_1}{\partial t} > 0$$

$$\Lambda^h = 0 \quad \text{if } \frac{\partial D_1}{\partial t} \leq 0$$

The so-called split-up method (*Marchuk, 1975*) is used to calculate the marine system equations. For first-order accuracy in time ($t_i \leq t \leq t_{i+1/2}$), the mass transport (advection and macroturbulence) is calculated. So,

$$\frac{\bar{c}_i^{t+1/2} - \bar{c}_i^t}{\Delta t} + \bar{\Lambda}_i \bar{c}_i^t = 0 \quad (14)$$

For second-order accuracy in time ($t_{i+1/2} \leq t \leq t_{i+1}$), the other terms of equations (11) and (13) are calculated:

$$\frac{\bar{c}_i^{t+1} - \bar{c}_i^{t+1/2}}{\Delta t} = \bar{F}_i^t \quad (15)$$

where: $\bar{\Lambda}_i$ is the finite-difference operator of \bar{L}_i .

2.2 Calculation of the thickness of the upper mixed layer and the variation in sea level

In the present two-dimensional model, the thickness of the upper mixed layer is dependent on space and time and is determined by an evolution equation in the following way:

$$\frac{\partial D_1}{\partial t} = -\varepsilon \frac{H - D_1}{\bar{b}_1 - \bar{b}_2} \frac{R_b}{D_1} \quad (16)$$

The calculation is separated into two different cases: the mixed layer is increasing ($\partial D_1 / \partial t > 0$) and the mixed layer is decreasing ($\partial D_1 / \partial t \leq 0$). For details see *Tamsalu and Myrberg* (1995). If the mixed layer is increasing, we have:

$$R_b = 2 \left(q_{b0} - \frac{m_1 u_*^3}{D_1} + \frac{\alpha_1 I_0}{c_p \rho_0} \left(1 + \frac{1}{\gamma D_1} e^{-\gamma D_1} \right) \right) \quad (17)$$

$$q_{b0} = \langle w' b' \rangle_0 = \alpha_1 q_{T0} - \beta q_{S0}, \quad \alpha_1 = \alpha (T_1 - T_0), \quad \varepsilon = 1.0$$

where: m_1 is a constant, u_* is the friction coefficient.

If the mixed layer is decreasing, we have $\varepsilon = 0.4$ and R_b takes the form:

$$R_b = q_{b0} \quad (18)$$

For the water level variation Z an evolution equation is determined:

$$\text{div}[\bar{u}_1 D_1 + \bar{u}_2 (H - D_1)] = \frac{\partial Z}{\partial t} \quad (19)$$

Finite-difference equations are composed using *Mesinger's* (1981) schemes.

3. Main characteristics of the Gulf of Finland hydrodynamics

The Gulf of Finland is a large estuarine basin having no sill with the Baltic Proper. Its surface area is 29 571 km², mean depth 37 m and volume 1103 km³. The length of the GOF is about 400 km and the width varies between 48-135 km. The greatest depth is 123 m (see *Falkenmark and Mikulski, 1975, Astok and Mälkki, 1988.*) The central gulf is quite deep up to longitude 28 degrees east. The southeastern part is somewhat shallower and the easternmost end of the gulf is very shallow. The southern coast is rather steep whereas the northern coast is very broken with small islands. The GOF gets narrow towards the eastern end after the large basin at longitude 28 degrees east. The Neva bight is a very narrow and shallow area. The topographic features are very rich and can be expected to have important effects on the circulations of the GOF.

The most striking feature of the hydrography of the GOF is that there is no specific physical border between the Baltic Sea Proper and the GOF, such as a narrower part or a shallower area. A line between the Hanko Peninsula and Osmussaari is conventionally treated as a border (see, e.g. *Witting, 1910*). In general, fresh water flows outwards from the GOF in the surface layer. The fresh water input into the GOF from rivers is an important factor causing water movements. It is of special importance in

spring, when river runoffs have their annual maximum and, on the other hand, the wind and atmospheric pressure gradients are weak. In autumn the fresh water input is smaller and strong southwesterly winds dominate. There is then on average an inflow of water along the southern coast and an outflow along the northern coast. The salty water from the Baltic Proper tends to penetrate into the GOF along the bottom. In the westernmost GOF near the Estonian coast there is a quasistationary salinity front close to the bottom. It has been estimated that the water in the GOF is renewed approximately every three years. The amount of fresh water coming in as river runoff is on average 114 km^3 yearly. This is about 25 percent of the whole fresh water input to the Baltic Sea, which shows how diverse the water masses of the GOF are. In general it can thus be concluded that the GOF is characterized by two water exchange processes; one at each end: the exchange with the Baltic Proper in the west, and the largest single fresh water input to the whole Baltic Sea from the river Neva, with a monthly mean discharge of $2700 \text{ m}^3/\text{s}$, in the east. The Neva dominates the physics at the eastern end of the GOF. The Neva discharge has a large yearly variability. In 1992, the year whose data are used in this paper, the minimum runoff of the River Neva was $1490 \text{ m}^3/\text{s}$ in January, while the maximum runoff was $3610 \text{ m}^3/\text{s}$ in June. Other rivers (Kymi, Narva, Luga) on both sides of the eastern GOF contribute to the fresh water supply as well. The Kymi and Narva rivers both have a yearly mean runoff of $300\text{-}400 \text{ m}^3/\text{s}$, while that of the Luga is about $100 \text{ m}^3/\text{s}$. The role of other rivers is negligible. The hydrography of the GOF is also modified by air-sea-interaction (wind stress, heat and vapour exchange), baroclinic effects (fronts), bottom topography, coastal effects and by the coriolis-effect. The circulation physics of the GOF have been studied in detail e.g. by *Witting* (1912), *Palmén* (1930), *Hela* (1952) and *Sarkkula* (1989).

It should be pointed out that salinity plays an important role in the buoyancy-driven currents in the Baltic Sea, whereas in the oceans temperature differences make larger contributions to buoyancy (see e.g. *Mälkki and Tamsalu*, 1985). This is the reason why special attention is paid in this study to a detailed analysis of the distribution of salinity.

4. *Material and methods*

4.1 *Initial conditions, data and parameter values*

Before the main simulations the model was initialized in the following way. Firstly, a climatological structure of salinity and temperature was given for the upper layer and for the bottom layer (*Bock*, 1971). After that a simulation of 5 years was carried out using realistic atmospheric, river water and water level input in order to be sure that the model had adapted to the real conditions of the year 1992 as well as to see that the model's numerical scheme was stable. Each of the simulations described later in this section was started using the abovementioned initial conditions, which are the

result of this 5 years' simulation. The main simulation period was from April 15 to September 3, 1992, when the measurements ended. It should be pointed out that the conclusions about the model simulations are based not only on the figures shown, but also on many other results not shown in this paper.

The monthly mean runoffs of the main rivers in the Gulf of Finland (Neva, Narva, Kymi, Luga) were used. The runoffs of the small rivers were added to the previously-mentioned river runoffs. Using the runoff data, Fourier coefficients were calculated to describe the time-dependency of river runoff.

In the first simulations, atmospheric data (6h intervals) from the automatic weather station of Kalbådagrund (59 deg. 58 min.N, 25 deg. 37 min.E) were used. The following meteorological parameters were used: wind speed and direction, atmospheric temperature, relative humidity and total cloudiness. Since cloudiness is not observed at Kalbådagrund, which is an automatic weather station, the values from the Isosaari weather station (60 deg. 07 min.N, 25 deg. 03 min.E) were used. The wind is measured at a height of 35 m. A 10 m wind speed was calculated according to the logarithmic wind law. In the latter simulations, input from the HIRLAM atmospheric model was used (see section 4.2).

The model simulations were mainly focused on August 1992, when 130 CTD observations were carried out on board R/V Aranda using a Neil Brown Mark III sonde. Unfortunately, during that year no current measurements were carried out by the Finnish Institute of Marine Research (FIMR). From the CTD measurements in the transition area between the Baltic Proper and the Gulf of Finland (longitude 22 deg.E), the boundary conditions for surface and bottom salinity were calculated. The measured water levels at Hanko and Heltermaa were used for assimilation of the water level on the western boundary of the model. The ability of the model to forecast water levels in other parts of the GOF was tested by comparing the model results with the water level observations from Helsinki and Hamina.

No current measurement field experiments were carried out in FIMR during 1992. The current measurement campaigns have been concentrated in the years 1994-1996. These current profiles will be later compared with the results of the three-dimensional model version (*Tamsalu*, 1996). Current measurements have been carried out during the 1990's in the Finnish Environmental Agency (*J. Sarkkula*, personal communication). However, the data have not yet been published.

The following model parameters were used in all simulations: grid step $dx=dy=4663$ m, time step $dt=10$ min, bottom friction $R = 1.5 * 10^{-3} * \sqrt{u_2^2 + v_2^2}$, coefficient of macroturbulence $\mu = 1 * 10^{-3} * dx^{4/3}$, coriolis-parameter $f = 2\bar{\omega} \sin \phi$; and drag-coefficient $C_d = (0.63 + 0.066 * U_{10})$, where U_{10} is the wind speed (m/s) at a height of 10 metres, ϕ is the latitude (rad), $\bar{\omega}$ is the angular velocity of the earth's rotation (rad s⁻¹).

4.2 *The use of meteorological forcing from the HIRLAM model*

The atmospheric model used in this paper is known as HIRLAM (**H**igh **R**esolution **L**imited **A**rea **M**odelling). This originally joint Nordic-Dutch model was developed in the 1980's (*Machenhauer, 1988*). The HIRLAM1 version has been in operational use in the Finnish Meteorological Institute (FMI) since January 1, 1990. Operational use of the HIRLAM2 version began in the FMI on June 1, 1994. The HIRLAM1 model version (*Gustafsson, 1991*) has a horizontal resolution of 0.5 degrees (latitude) and 1.0 degrees (longitude), which translates to about 55*55 km in the Baltic Sea area. The HIRLAM1 version has about 30 vertical levels. During 1995 a model version with a resolution of about 25*25 km was brought into use in the FMI.

The output fields (6h forecasts) from the HIRLAM model (wind speed and direction, atmospheric temperature) were further modified to be usable for the sea model. An areal interpolation was carried out in order to place the HIRLAM data on the grid of the sea model (*Cheng and Launiainen, 1993*). The horizontal resolution of the sea model is about 5 minutes (longitude) and 2.5 minutes (latitude), which means about 4.5*4.5 kilometres. The interpolated HIRLAM winds from the lowest model level, namely at a height of 32-35 m, were compared with the measured winds at Kalbådgrund (35 m height), which is nowadays the only true open-sea station in the GOF. The comparisons showed that the modelled winds speeds were in general lower than those observed (Fig. 1A). This difference can most probably be explained by the lack of resolution of the HIRLAM model. The model can not "see" the Gulf of Finland. The areal interpolation of the winds also causes some reduction of the speeds, because HIRLAM grid points near the coast are used in this procedure. The total number of grid points used is only about 15.

A simple correction to the interpolated HIRLAM winds speeds for the whole year 1992 is carried out. The corrections to the HIRLAM wind fields only affect wind speed. Corrections to wind direction are too complicated, and besides, the wind direction is mainly determined by the surface pressure pattern, which is well enough forecasted by the HIRLAM model (Fig. 1A). Atmospheric temperature corrections are not carried out because of the lack of observations over the open sea needed to describe the complicated temperature pattern.

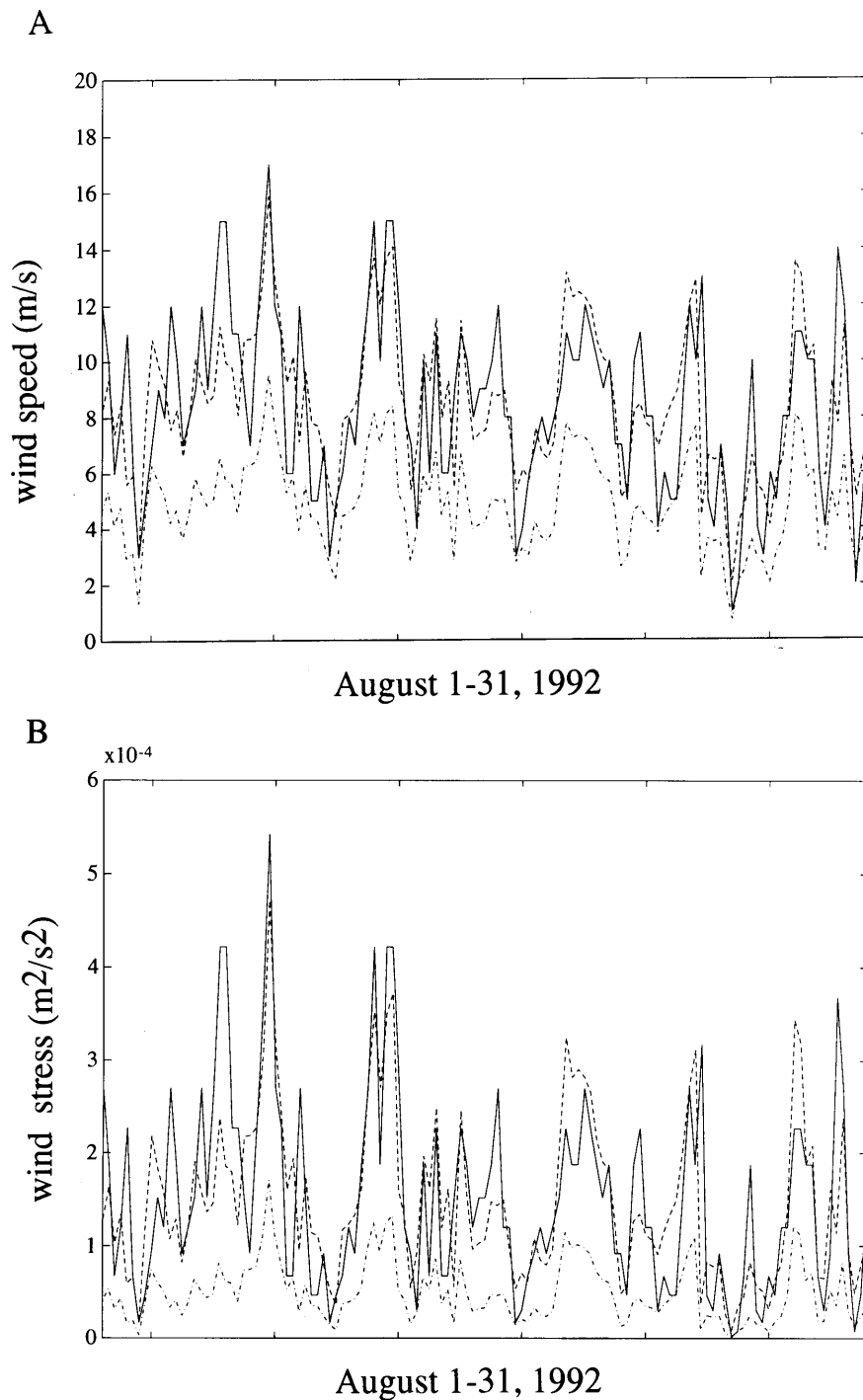


Fig. 1. The time evolution of wind speed in m/s (A) and wind stress (B) in m^2 / s^2 during August 1-31, 1992 at the Kalbådagrund weather station in the Gulf of Finland. The measured wind speeds and wind stresses at Kalbådagrund are marked with continuous lines, the interpolated HIRLAM parameters with dash-dotted lines, and the corrected (by Eq. 20) interpolated HIRLAM parameters with dashed lines.

4.2.1 Corrected HIRLAM wind fields

A regression analysis is used to correct the HIRLAM wind speeds by taking the measured winds speeds at Kalbådagrund as the correct values. Measurements at 6h

intervals at Kalbådagrund (00, 06, 12, 18 GMT) are used to correct the corresponding HIRLAM wind fields. The following first-order regression equation employed is

$$U_{corr}^{HIRLAM} = a_0 + a_1 U^{HIRLAM} \quad (20)$$

where: U^{HIRLAM} is the original HIRLAM wind speed (m/s), U_{corr}^{HIRLAM} is the corrected HIRLAM wind speed (m/s), $a_0=1.0$, $a_1=1.5$.

The original HIRLAM winds at the location of Kalbådagrund are corrected using (20). The results are shown in Figure 1A. The corrected HIRLAM winds are quite accurate. The mean ratio K between the wind stress calculated from the Kalbådagrund winds and that calculated from the interpolated HIRLAM winds has been determined using the wind data of every 6h. K found to be 4. If the corrected interpolated HIRLAM winds are used, K equals 1.1, which means that at least the mean wind stress is accurate. (Fig. 1B).

The HIRLAM wind fields discussed here are from a height of about 35 m. The 10 m winds are calculated from the 35 m winds as follows (*T. Vihma*, personal communication):

$$U_{10m} = 0.9U_{35m} \quad \text{if } Ri \leq 0 \quad (21a)$$

$$U_{10m} = (0.9 - 0.5Ri)U_{35m} \quad \text{if } Ri \geq 0 \quad (21b)$$

where:

Ri , the non-dimensional Richardson number, is given by:

$$Ri = \frac{gZ}{T_{35m}} \frac{(T_{35m} - T_s)}{U_{35m}^2} \quad (22)$$

Here, U_{35} (m/s) is the corrected HIRLAM wind speed at a height of 35 m, U_{10} is the calculated HIRLAM wind speed at a height of 10 m, T_{35m} (degrees K) is the HIRLAM air temperature at a height of 35 m and T_s is the sea-surface temperature calculated by the sea model, $Z=35$ m.

Products of relative humidity and total cloudiness are not easily available from HIRLAM. So, those values measured at a single station have also been used throughout the HIRLAM simulations.

According to *Launiainen and Saarinen* (1982) there can be major differences between the wind speeds in an open sea-area and in the coastal area. The wind direction affects the differences of wind speed between coastal and open sea-areas through variable roughness and orographic effects. The atmospheric surface layer stability also affects the wind speed differences. Due to the low resolution of the model, the HIRLAM winds for open-sea and coastal areas do not differ much from each other. It is

therefore possible that the interpolated HIRLAM winds in the coastal areas, when the correction by (20) has been made, are slightly overestimated compared with the real winds there. However, use of the interpolated HIRLAM winds in coastal areas is certainly more realistic than using the space-independent winds from Kalbådagrund. On the other hand, the interpolation procedure slightly decreases the HIRLAM winds in the open sea-area compared with the HIRLAM winds in the original grid system.

4.3 *Weather conditions in the Gulf of Finland in August 1992*

At the beginning of August (*Helminen, 1992*) a weak high pressure centre was located south of Finland and the weather was clear but not very warm. The air temperature at Kalbådagrund varied between 13-20 °C, while the wind speed there was between 5-10 m/s, with the wind blowing on average from the west. Between 4 and 7 August two frontal systems moved over Finland. In connection with this, high winds of between 10-17 m/s from the west were observed. The weather remained quite warm during this period. Between 8 and 10 August the weather was relatively cold with light winds from the northwest. On August 10 very warm air was advected to Finland and record temperatures for summer 1992 were achieved on August 11. Light southerly winds were observed. After that, the weather became cooler and high winds of up to 20 m/s from the southwest were observed on August 13. Temperatures fell from more than 25 °C on August 11 down to 11 °C on August 20. The diurnal temperature variability was small. After August 20 a high pressure centre formed over Finland, but the weather was cold and cloudy with moderate northerly winds. During the last part of the month the weather was quite changeable. On August 24 and 28 frontal systems arrived in Finland from the west and the wind direction varied between east and west. Wind speeds were usually below 10 m/s, occasionally being 12-14 m/s. Temperatures were near 14 °C and the diurnal variability of temperature was small. During the last days of August a weak high pressure centre formed over Finland. Winds turned from westerly to easterly and advection brought warm air from the east.

5. *The model simulations*

5.1 *Comparison of the model results with different meteorological forcings*

In this section the model results for salinity, temperature, the thickness of the upper mixed layer and water level height will be compared with measurements. The first model version, in which atmospheric forcing derived from Kalbådagrund observations is used, will be referred to the **2DK**-model. The second model version, in which the air temperature and wind stress fields are obtained from the HIRLAM model, will be referred to the **2DH**-model.

5.1.1 *Surface salinity fields*

The overall horizontal structure of salinity given by the 2DK model (Fig. 2A) is generally in accordance with measurements. The surface salinity varies from about 6.5 PSU in the southwestern part to about 0.5 PSU in the mouth of River Neva. The effects of fresh water input from the Kymi, Narva and Luga rivers are also clearly visible. In the western part of the Gulf the errors in the 2DK prognoses are of the order of ± 0.2 PSU (Fig. 2A). In the eastern part of the central Gulf the 2DK model (Fig. 2A) gives salinities which are systematically about 0.7-1.0 higher than the measurements. In the western part of the central Gulf the 2DK model overestimates the salinity by 0.4-1 PSU. In the eastern Gulf the model overestimates the salinity by about 1 PSU.

The 2DH model gives better results than the 2DK model in all parts of the Gulf (Fig. 2B; see section 5.1.3). In the eastern part of the central Gulf the 2DH model gives very good results with errors of ± 0.2 PSU. In the western part of the central Gulf an overestimation of 0.1-0.7 PSU is still evident even in the 2DH-model. The most pronounced differences between the 2DH and 2DK models are in the eastern Gulf of Finland, where the 2DK model (Fig. 2A) gives e.g. on August 18 a value of 3.5 PSU, while the 2DH model (Fig. 2B) gives 2.7 PSU. The measured value at that point (station F40; 60 deg. 06 min.N, 28 deg. 48 min.E.) was 2.3 PSU.

The time evolution of salinity in the western part of the GOF (station GR6, 59 deg. 41 min.N, 23 deg. 34 min.E), shows the role played by the fixed values for salinity at the model's western boundary (not shown). The surface salinity variability according to the model results is less than that shown by measurements.

5.1.2 *Surface temperature fields*

Surface temperature fields simulated by the 2DK model (Fig. 3A) show that the horizontal temperature gradients are very small. This can be simply explained by the fact that the spatial variability of air temperature was not taken into account (see section 4.1-4.2). The 2DK model overestimates the surface temperature up to the middle of August by about 0.5-1.5 degrees. During the second half of August the model underestimated the temperature by about 1-2 degrees (Fig. 3A), even by as much as 4 degrees on August 22. The model's ability to describe the sea-surface temperature is thus only moderate if atmospheric input from a single point is used.

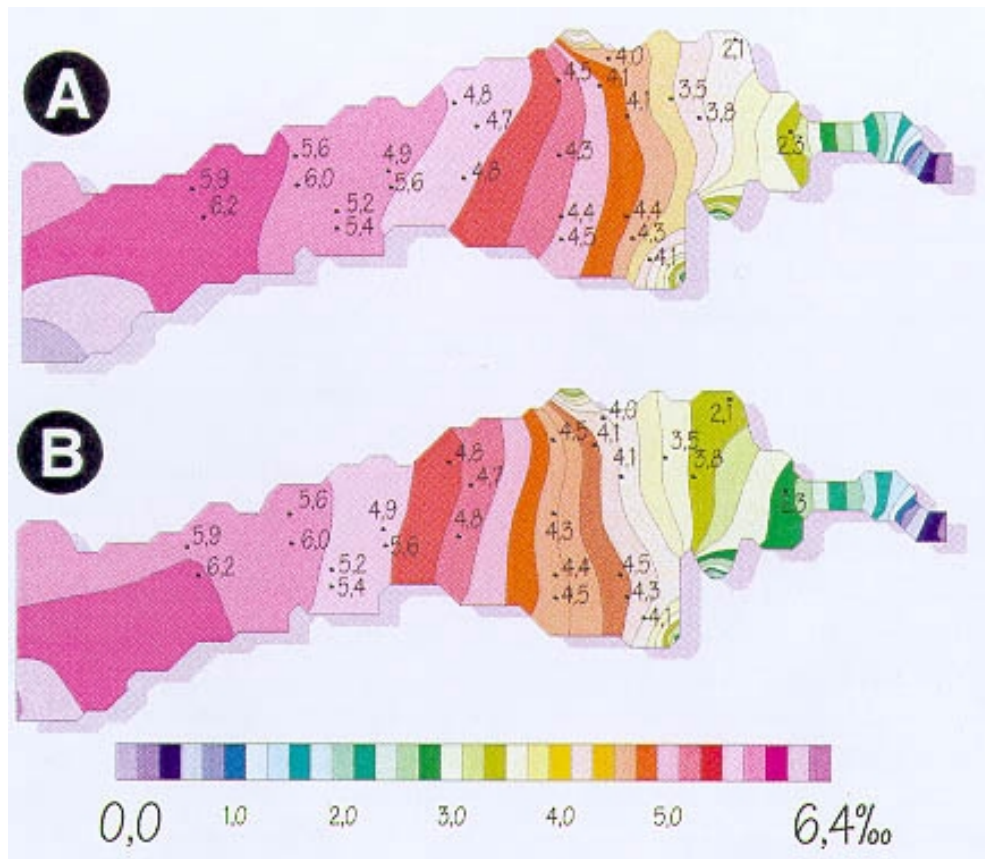


Fig. 2. Surface salinity fields in the Gulf of Finland. (A): simulated by the 2DK model version using the atmospheric forcing derived from the Kalbådagrund weather station and (B): simulated by the 2DH model version using the atmospheric forcing from HIRLAM. The figures represent the mean of model results from August 18-21. Positions of the salinity measurements carried out between August 18-21 are marked with a black dot (according to model results changes in the horizontal salinity field were small during August 18-21). The isoline analysis of the model results is shown at intervals of 0.2 PSU and the scale of the corresponding colours are shown below.

The 2DH model results show more pronounced sea temperature gradients than those from the 2DK. However, the simulated sea temperature results of the 2DH model are not much more accurate than the 2DK model results (Fig. 3B; see section 5.1.3). At the beginning of August (up to August 5) the 2DH model overestimates the temperatures by about 0.3-1 degrees. After that, up to August 15, the 2DH model results have errors of about ± 1 degrees. In late August the 2DH model overestimates the temperature by about 1-2 degrees.

The time-evolution of sea temperature in the upper mixed layer at station LL9 (59 deg. 42 min.N, 24 deg. 02 min.E) from early May up to the beginning of September shows that the 2DH model is capable of reproducing the seasonal time evolution of temperature in the GOF (not shown). The large error in the model results around May 20 can be explained by the difficulties in the determination of the evolution of the upper

mixed layer in spring. The time-evolution of sea temperature is well forecasted at station GR7 (59 deg. 34 min.N, 23 deg. 34 min.E), which is located in the western part

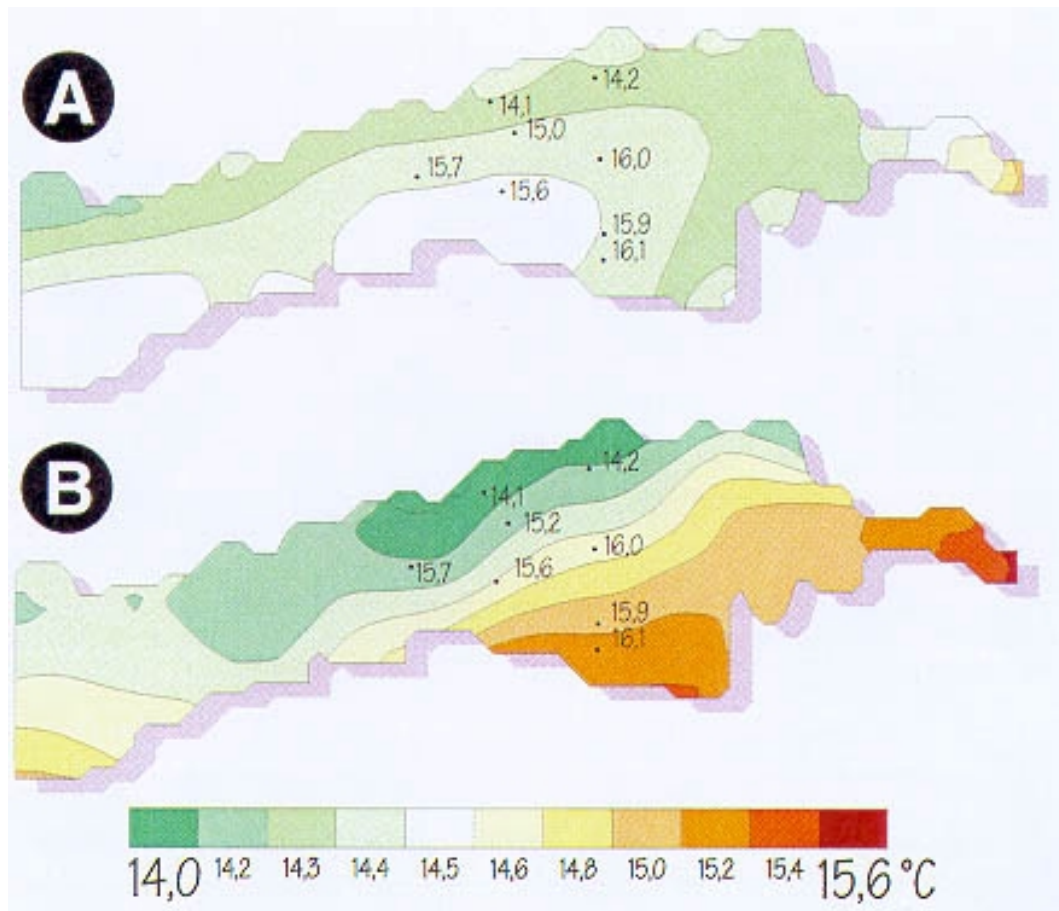


Fig. 3. Surface temperature field in the Gulf of Finland. (A): simulated by the 2DK model version using the atmospheric forcing derived from the Kalbådagrund weather station and (B): simulated by the 2DH model version using the atmospheric forcing from HIRLAM. The figures represent the situation on August 20 at 12 GMT. Observed values are marked by a black dot with the corresponding value. The isoline analysis of the model results is shown at intervals of 0.1 degrees (A) and of 0.2 degrees (B) and the scale of the corresponding colours is shown below.

of the GOF (not shown). However, at a station closer to the Finnish coast, i.e. GR6 (59 deg. 41 min.N, 23 deg. 34 min.E), an upwelling most probably took place on August 7, when a strong westerly wind of about 17 m/s was observed. This upwelling feature was not properly forecasted by the model (Fig. 4). In general, the sea-temperature difference between the 2DH and 2DK models is at most 3 degrees, usually 0-1 degrees. The 2DH model usually gives somewhat higher temperatures than the 2DK. This is because the HIRLAM daily air temperatures (amplitudes) are often higher compared to those observed, especially near the coasts.

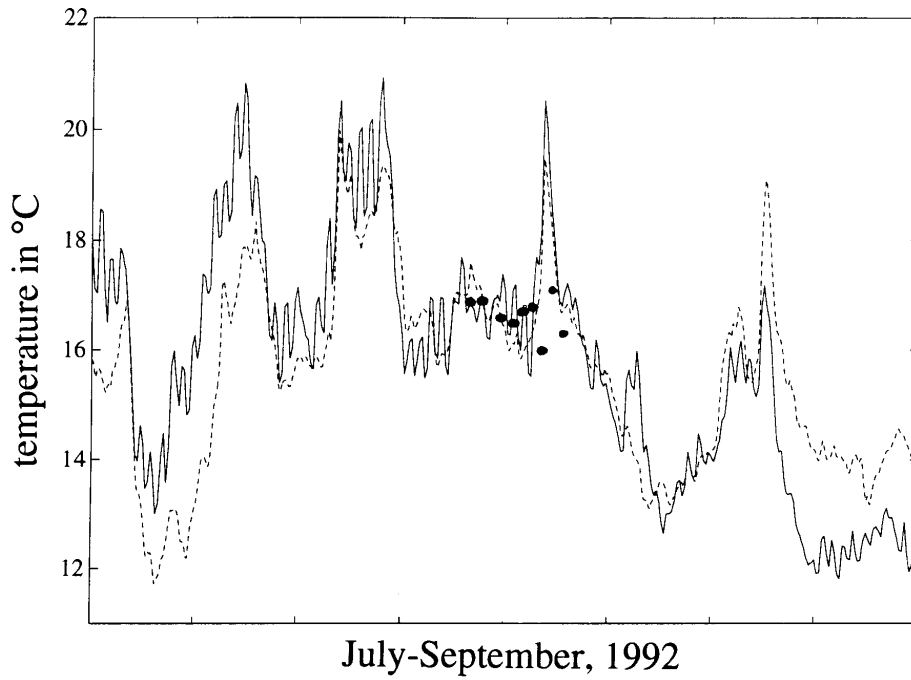


Fig. 4. Time evolution of temperature in the upper mixed layer at station GR6 (59 deg. 41 min.N, 23 deg. 34 min.E). The continuous line represents results as simulated by the 2DH model, the broken line those of the 2DK model.

5.1.3 Statistical analysis

A statistical analysis was carried out in order to investigate how reliable the model results are compared with observations, and besides this to see whether the use of the HIRLAM atmospheric model has any effect in reducing the errors of model results compared with observations. The statistical error R (as a percentage) is defined as follows:

$$R = 100 \frac{\sum_{i=1}^n \text{abs}(F_{MO} - F_{ME})_i / n}{\bar{F}_{ME}} \quad (23)$$

$$\bar{F}_{ME} = \sum_{i=1}^n (F_{ME})_i / n$$

where:

R is the error as a percentage, F_{ME} is the value of the measured variable (surface salinity or temperature) at an observational point, F_{MO} is the value of the variable simulated by the model at the same location, \bar{F}_{ME} is the mean of all the observations of

the variable in the studied area, n is the number of observations ($n=130$ for the whole GOF).

In Tables 1A and 1B, the errors have been given for surface salinity and temperature found when using the 2DK and the 2DH models. The errors have been calculated separately for the western GOF, the central GOF, the eastern GOF and for the whole GOF. The number n in (23) is here the number of observations in the corresponding sea-area.

Table 1a. The error R (as a percentage) in surface salinity simulations produced by the 2DK and the 2DH models for various parts of the GOF: the western GOF, the central GOF, the eastern GOF and the whole GOF.

	WGOF	CGOF	EGOF	whole GOF
2DK	2.5	13.1	27.5	7.3
2DH	2.0	6.0	10.0	4.0

Table 1b. The error R (as a percentage) in surface temperature simulations produced by the 2DK and the 2DH models for various parts of the GOF. In temperature calculations the Celsius scale has been used.

	WGOF	EGOF	CGOF	whole GOF
2DK	5.3	7.6	8.3	6.0
2DH	4.2	6.7	8.3	5.6

The statistical error analysis shows clearly that the 2DH model gives better results for surface salinity than 2DK (errors 4.0 % versus 7.3 %). The difference between these models is smallest in the westernmost GOF (2.0 % versus 2.5 %) because the salinity has a constant value at the western boundary. The difference in accuracy between the 2DK and the 2DH models' salinity simulations increases eastwards, because the dominating effect of the fixed western boundary is not important, besides which there are large salinity gradients in the central (errors 6.0 % versus 13.0 %) and the eastern GOF (errors 10.0 % versus 27.5 %), which can be predicted accurately only making use of the HIRLAM input.

The error analysis of surface temperature between the 2DK and the 2DH models shows no major difference in accuracy. The 2DH model is more accurate than the 2DK model (error for the whole of the GOF; 5.6 % versus 6.0%), except in the eastern part, where the results are equally accurate.

5.1.4 Thickness of the upper mixed layer

The results of the 2DK and the 2DH models for the thickness of the upper mixed layer are so similar that only the latter case is analyzed here. The model seems to be able to predict the mixed layer thickness in the open sea-area, where the errors in model results are about ± 3 metres. However, rapid changes in the thickness of the upper mixed

layer caused by upwellings, or by considerable cooling/warming in the atmosphere, cannot be forecast accurately. This is due partly to shortcomings in the model physics. In the model the upper mixed layer never vanishes, whereas during an upwelling the upper layer in fact does vanish (*Hela, 1976*). Thus, problems in determining the thickness of the upper layer are most pronounced near the coasts. To some extent the errors are also caused by inaccuracies in the atmospheric forcing. Figures 5A, B show how the water body in the eastern GOF becomes well-mixed between August 18-20 due to a cold air outbreak and its corresponding northerly winds (Fig. 1A; see section 4.3). This mixing seems to have some observational support.

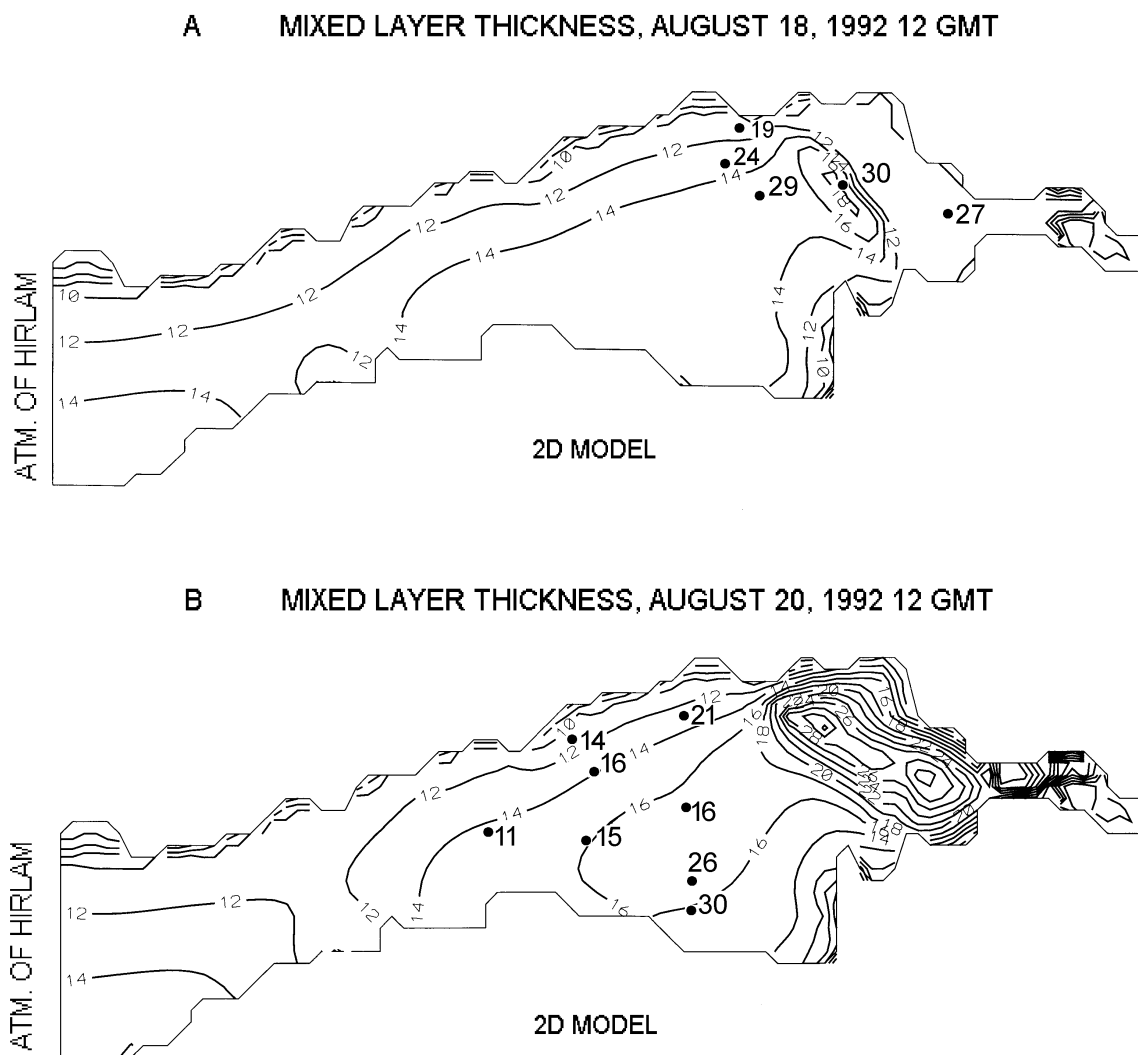


Fig. 5. Fields of the thickness of the upper mixed layer in the Gulf of Finland simulated by the 2DH model version. The figures represent the situation at 12 GMT each day: August 18 (A), August 20 (B). Observed values are shown by a black dot with the corresponding value. The isoline analysis of the model results is shown at intervals of 2 metres.

5.1.5 Currents and water level

A brief look at the current fields of the upper mixed layer (vertically integrated) show that there are some differences between the 2DK and the 2DH results (Figs. 6A, B). In cases of prevailing westerly winds, which was typically the situation in August 1992, the 2DK model-produced currents are stronger in coastal areas than those from 2DH. This can be explained by the overestimation of wind speed in the coastal areas in the 2DK model. The effects of the curl of wind stress becomes visible in the 2DH model results in terms of the more complicated horizontal current patterns including vortices etc. The 2DK model's tendency to transport water eastwards more effectively than the 2DH model is clear.

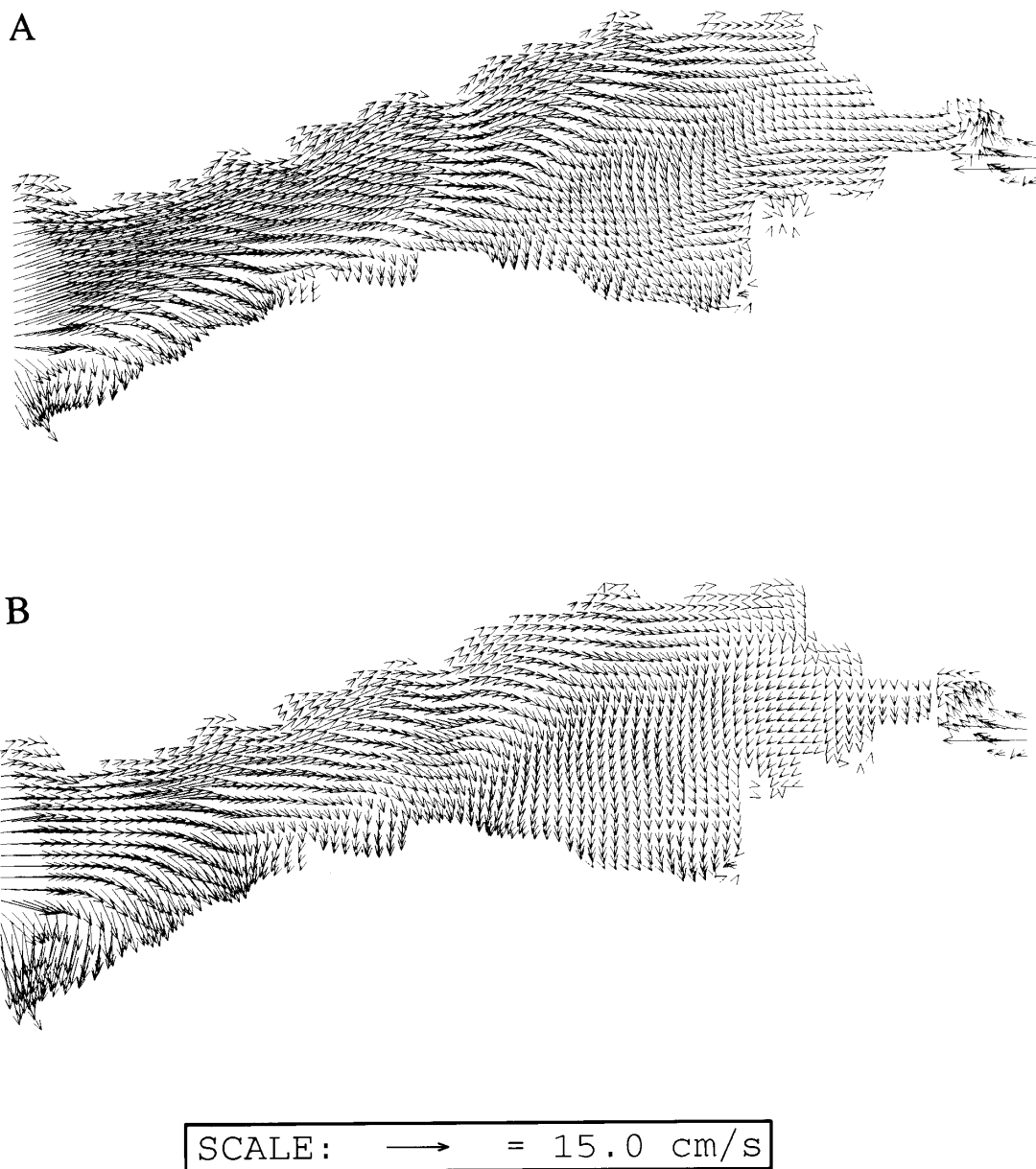


Fig. 6. Currents in the upper mixed layer of the Gulf of Finland. The figures represent the situation on August 27 at 12 GMT. (A): as simulated by the 2DK model, (B): as simulated by the 2DH model.

The water levels heights produced by the model were compared with observations from Helsinki and Hamina. In Figure 7, the water levels produced by the 2DK and by the 2DH models have been compared with observations from Hamina in August 1992. The 2DK and the 2DH model results clearly differ from each other to some extent, but which of them gives more accurate results is difficult to conclude. More important is the fact that the two-dimensional model is capable of reproducing the main features of water level variability. There seem to be no major phase differences between model results and measurements. The timing of water level maxima are well reproduced by the model even though the highest observed water levels are underestimated by it. The water level variation in Helsinki was also investigated. The results of the comparisons were quite the same as for Hamina.

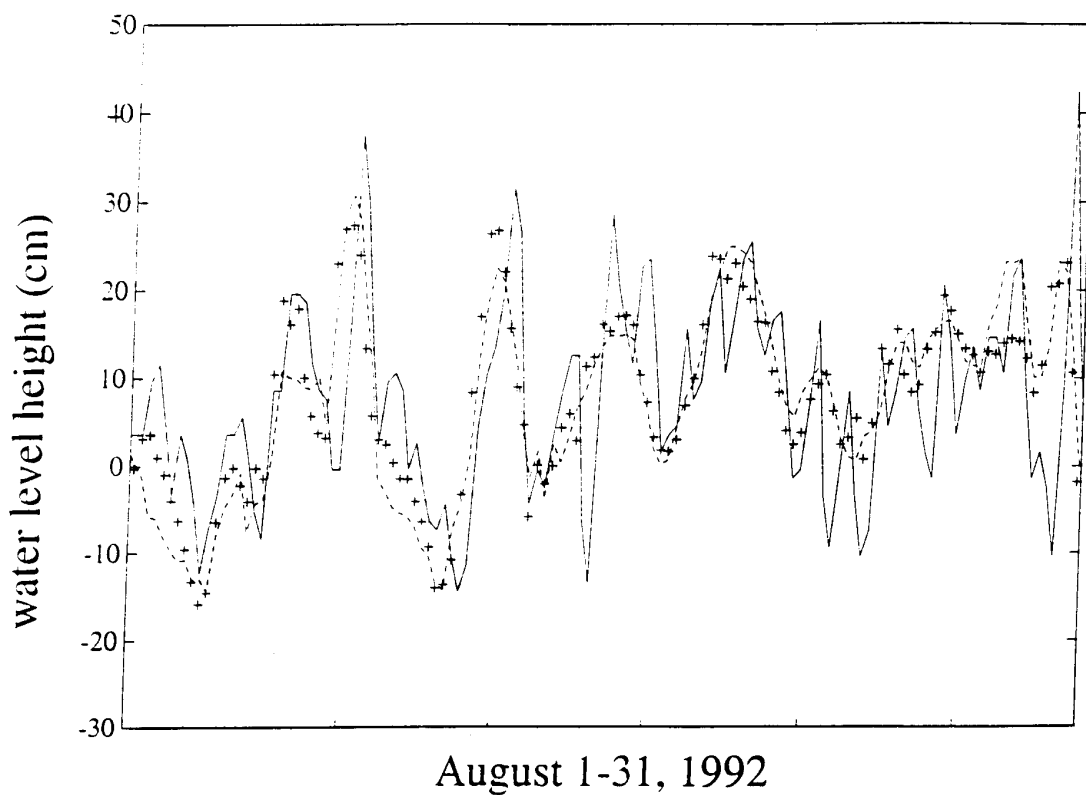


Fig. 7. Time evolution of water level height at the coastal station of Hamina (60 deg., 35 min.N, 27 deg., 10 min.E) in the Gulf of Finland on August 1-31, 1992. The measured water level is marked with a continuous line, the 2DK model results with + symbols and the 2DH model results with a broken line.

6. *Summary and conclusions*

A new version of a two-dimensional, two-layer baroclinic prognostic model for the Gulf of Finland has been developed and the model results have been compared with measurements of salinity, temperature, the thickness of the upper mixed layer and water level heights for summer 1992. The main idea was, on the one hand, to test whether the model is able to reliably reproduce the main physical features in the uppermost layer of

the GOF, and on the other hand to see what the effect of using space-dependent and space-independent atmospheric forcings is on the results of the marine hydrodynamic model.

The simulations of surface salinity showed satisfactorily the complicated horizontal structure with pronounced gradients. The fixed boundary values for salinity in the west became visible in the model results as too small a variability of salinity compared with measurements. The problem with open boundaries is a clear shortcoming in all regional models and leads to some limitations in their use. The employment of input from the HIRLAM atmospheric model clearly improved the model results in the eastern GOF. It is probable that the HIRLAM space-dependent wind fields better describe the situation over the eastern GOF than do the open sea winds of the Kalbådagrund weather station; strong westerly winds there cause too much eastward water transport and too strong mixing. As a result, the thin fresh water layer vanishes and the model overestimates the surface salinity. Due to the large fresh water input from the rivers, large horizontal gradients occur in the eastern GOF, so that the exact location of the fronts is sensitive to atmospheric forcing.

In the temperature simulations, the seasonal time-evolution of surface layer temperature was fairly well simulated by the model. However, there are clear differences between the 2DK and the 2DH models' results concerning horizontal fields of temperature. In the 2DK results, the horizontal variation of surface layer temperature was negligible, while in the 2DH results major gradients became visible. This is simply a consequence of the use of the spatially-variable atmospheric temperature in the latter simulation. However, the accuracy of the 2DH model results when compared with measurements is only slightly better than that of the 2DK model. This can be explained by the lack of resolution in the atmospheric model to describe the air temperature pattern accurately enough over the sea-area.

To some extent the thickness of the upper mixed layer can be predicted by the model over the open sea-area, but the consequences of local upwellings, warming/cooling of the atmosphere etc. are difficult to simulate with the two-dimensional model. The correct time and place of the production of a well-mixed sea in late August is difficult to reproduce and with it a forecast of the related abrupt changes in surface temperature and salinity. A proper modelling of upwelling needs a 3D model, in which the vertical velocity is calculated.

The current fields showed some interesting differences between the 2DK and the 2DH model results. When typical westerly winds dominate, the 2DK model seems to produce higher currents than the 2DH model in coastal areas, which is to be expected, because the wind measurements from Kalbådagrund overestimate the wind speed at the shoreline as well as in the eastern GOF. Thus the 2DK model also has a tendency to produce higher eastward current speeds in the eastern GOF than the 2DH model. This leads to an overestimation of surface salinity there. The overall time evolution and main peaks of the water level variations can be described by the present model. Atmospheric

forcing seems to play a certain role, but it is probable that the wind field at the shorelines is not so well described by the HIRLAM model that it could have a positive signal in the model results. The data-assimilation of water levels at the mouth of the GOF plays a crucial role in the models' ability to produce reliable water levels in the coastal areas of the GOF.

This study has shown that atmospheric models need still higher horizontal resolution in such narrow gulfs as the Gulf of Finland in order to describe the wind and temperature fields accurately. Today, the Finnish Meteorological Institute uses a version of the HIRLAM model in which the horizontal resolution is about 25*25 km. Hopefully this atmospheric input can soon be used in sea models.

The two-dimensional model has shown some possibilities for reproducing the main features of the hydrodynamics of the Gulf of Finland. In the near future the results of the two -and three-dimensional models will be compared with each other and with measurements in order to find out the main differences between the results of models representing a different order of complexity.

Acknowledgements

I would like to thank D.Sc. Rein Tamsalu for his guidance of this work and for his comments on the manuscript. I extend my appreciation to Dr. Timo Vihma for helping me in the surface parameterization of the HIRLAM winds, and to Mr. Kalle Eerola for making the HIRLAM data available. Mr. Bin Cheng and Prof. Jouko Launiainen have developed the atmospheric interpolation program, which is gratefully acknowledged, as are also the critical comments of the anonymous referees.

References

- Andrejev, O. and A. Sokolov, 1992. On the nested grid approach for the Baltic Sea numerical problem to solve. *Proceedings of the 18th Conference of the Baltic Oceanographers*, St. Petersburg, Russia, **Vol. 1**, 55-68.
- Andrejev, O., T. Babaeva, E. Chernysheva, A. Gusev, L. Kalinina, O. Savchuk, A. Sokolov and I. Tsuprova, 1992. 3D-dispersion of non-conservative substances in the Gulf of Finland. *Proceedings of the 18th Conference of the Baltic Oceanographers*, St. Petersburg, Russia, **Vol. 1**, 69-76.
- Astok, V. and P. Mälkki, 1988. Laht maailmakaardil. *Eesti Loodus* **9**, 554-558.
- Backhaus, J., 1985. A three-dimensional model for the simulation of shelf sea dynamics. *Dt. Hydrogr. Z.*, **38**, 165-187.
- Blumberg, A., 1977. Numerical tidal model of Chesapeake Bay. *J. Hydraul. Div.*, **103**, 1-10.

- Blumberg, A. and G. Mellor, 1987. A description of a three-dimensional coastal ocean circulation model. In: Three-dimensional coastal ocean models (ed., N. Heaps), *Coastal and Estuarine Sciences* **4**, 1-16. American Geophysical Society, Washington.
- Bock, K., 1971. Monatskarten des Salzgehaltes der Ostsee, dargestellt für verschiedene Tiefenhorizonte. *Dt. Hydrogr. Z., Ergänzungsheft Reiche B* **12**, 1-147.
- Bryan, K., 1969. A numerical method for the study of the circulation of the World Ocean. *J. Comput. Phys.*, **4**, 347-376.
- Cheng, B. and J. Launiainen, 1993. Use of an atmospheric model (HIRLAM) data as an input for marine studies and models. *Finnish Institute of Marine Research, Internal report* **14**, Helsinki, 9 pp.
- Chilika, Z., 1984. Verification of a certain numerical model with real storm surge of December 1976 in the Baltic Sea. *Oceanologia* **19**, 25-42.
- Chilika, Z. and Z. Kowalik, 1984. Influence of water exchange between the Baltic Sea and the North Sea on storm surges in the Baltic. *Oceanologia* **19**, 5-23.
- Davies, A., 1980. Application of the Galerkin method to the formulation of a three-dimensional nonlinear hydrodynamic numerical sea model. *Appl. Math. Modell.*, **4**, 245-256.
- Davies, A., 1994. On the complementary nature of observational data, scientific understanding and model complexity: the need for a range of models. *J. Marine Systems*, **5**, 406-408.
- Elken, J., 1994. Numerical study of fronts between the Baltic sub-basins. *Proceedings of the 19th Conference of the Baltic Oceanographers*, Sopot, Poland, **Vol. 1**, 438-446.
- Falkenmark, M. and Z. Mikulski, 1975. The Baltic Sea - a semi-enclosed sea, as seen by the hydrologist. *Nordic Hydrology*, **6**, 115-136.
- Funkquist, L. and L. Gidhagen, 1984. A model for the pollution studies in the Baltic Sea. *SMHI Reports, Hydrology and Oceanography*, RHO **39**, Norrköping.
- Gustafsson, N., 1991. Numerical methods in atmospheric models. *ECMWF proceedings*, 9-13 September, 1991, **Vol. 2**, 115-145, Reading.
- Hansen, W., 1956. Theorie zur Errechnung des wasserstandes und der Strömungen in Randmeeren nebst Anwendungen. *Tellus*, **8**, 287-300.
- Heaps, N., 1985. Tides, storm surges and coastal circulations. In: *Offshore and coastal modelling*. Lecture notes on coastal and estuarine studies **12**, Springer-Verlag, Berlin.
- Hela, I., 1952. Drift currents and permanent flow. *Soc. Sci. Fenn. Commentationes Physico-Mathematicae*, XVI. **14.**, Helsinki, 27 pp.
- Hela, I., 1976. Vertical velocity of the upwelling in the sea. *Soc. Sci. Fenn. Commentationes Physico-Mathematicae*, **46**(1), 9-24, Helsinki.
- Helminen, J. (ed), 1992. Kuukausikatsaus Suomen ilmastoon, elokuu 1992. Ilmatieteen laitos, Helsinki.

- Häkkinen, S., 1980. Computation of sea level variations during December 1975 and 1 to 17 September 1977 using numerical models of the Baltic Sea. *Dt. Hydrogr. Z.*, **33**.
- Jokinen, O., 1977. Hansenin yksikerrosmallin sovellutuksia. Geofysiikan päivät 10-11.3.1977, Helsinki (in Finnish).
- Kielmann, J., 1981. Grundlagen und Anwendung ein numerischen Modells der geschichteten Ostsee. Teil 1 und 2. *Berichte aus dem Institute für Meereskunde an der Universität Kiel*, No. **87**, Kiel.
- Killworth, P., D. Stainworth, D. Webbs and S. Paterson, 1991. The development of a free-surface Bryan-Cox-Semtner-Killworth ocean model. *J. Phys. Oceanogr.*, **21**, 1333-1348.
- Klevanny, K., 1994. Simulation of storm surges in the Baltic Sea using an integrated modelling system 'CARDINAL'. *Proceedings of the 19th Conference of the Baltic Oceanographers*, Sopot, Poland, **Vol. 1**, 328-336
- Koponen, J., 1984. Vesistöjen 3-dimensioinen virtaus- ja vedenlaatumalli. Diplomityö, Teknillinen Korkeakoulu, Otaniemi, 97 pp. (in Finnish).
- Koponen, J., M. Virtanen, H. Vepsä and E. Alasaarela, 1994. Operational model and its validation with drift tests in water areas around the Baltic Sea. *Water Poll. Res. J. Canada*, **29**, Nos. 2/3, 293-307.
- Kowalik, Z., 1969. Wind-driven circulation in a shallow sea with application to the Baltic Sea. *Acta Geophysica Polonica*, **17**, 13-38.
- Kowalik, Z., 1972. Wind-driven circulation in a shallow stratified sea. *Dt. Hydrogr. Z.*, **25**, 265-278.
- Kowalik, Z. and A. Staskiewicz, 1976. Water exchange between the Baltic and North Sea based on a barotropic model. *Acta Geophysica Polonica*, **24**, 310-315.
- Kowalik, Z. and T. Murty, 1993. Numerical modeling of ocean dynamics. *Advanced Series on Ocean Engineering*, **5**. World Scientific Publishing Co., Singapore, 481 pp.
- Krauss, W. and B. Brügge, 1991. Wind-produced water exchange between deep basins of the Baltic Sea. *J. Phys. Oceanogr.*, **21**, 373-384.
- Laska, M., 1966. The prediction problem of storm surge in the southern Baltic based on numerical circulations. *Archiwum Hydrotechniki* **13**, 335-366.
- Laevastu, T., 1973. A multilayer hydrodynamical model of type W. Hansen. Environmental Prediction Research Facility, Monterey.
- Launiainen, J. and J. Saarinen, 1982. Examples of comparison of wind and air-sea interaction characteristics on the open sea and in the coastal area of the Gulf of Finland. *Geophysica*, **19**(1), 33-46.
- Lehmann, A., 1995. A three-dimensional baroclinic eddy-resolving model of the Baltic Sea. *Tellus*, **47**, 1013-1031.
- Machenhauer, B., 1988. The HIRLAM Final Report. *HIRLAM Technical Report*, No. **5**, DMI, Copenhagen, Denmark, 116 pp.

- Marchuk, G., 1975. Numerical methods in weather prediction. Academic Press, New York, 277 pp.
- Mesinger, F., 1981. Horizontal advection schemes of a staggered grid -a enstrophy and energy conserving model. *Mon. Wea. Rew.*, **109**, 467-478.
- Miropolski, Y., 1981. Dynamics of internal gravity waves in the ocean, Moscow, 300 pp. (in Russian).
- Müller-Navarra, S., 1983. Modellergebnisse zu baroklinen Zirkulation im Kattegat, im Sund und in der Beltsee. *Dt. Hydrogr. Z.*, **36**, 237-257.
- Myrberg, K., 1992. A two-layer model of the Baltic Sea. Phil.lic. thesis. University of Helsinki, Department of Geophysics, Helsinki, 132 pp.
- Mälkki, P. and R. Tamsalu, 1985. Physical features of the Baltic Sea. *Finnish. Mar. Res.*, **252**, 110 pp, Helsinki.
- Nihoul, J. (ed.), 1982. Hydrodynamics of semi-enclosed seas. Elsevier Oceanography Series, **34**, Amsterdam, 555 pp.
- Nihoul, J. and B. Jamart, 1987. Three-dimensional models of marine and estuarine dynamics. Elsevier Oceanography Series, **45**, Amsterdam, 629 pp.
- Nihoul, J., 1994. Do not use a simple model when a complex one will do. *J. Marine Systems*, **5**, 401-406.
- Niiler, P. and E. Kraus, 1977. One dimensional models of the upper ocean. In: *Modelling and prediction of the upper layers of the ocean* (ed. E.Kraus), Pergamon Press, Oxford, 143-172.
- Oberhuber, J., 1993. Simulation of the Atlantic circulation with a coupled sea ice-mixed layer-isopycnal general circulation model. Part I: Model description. *J. Phys. Oceanogr.*, **23**, 808-829.
- O'Brien, J., 1967. The non-linear response of a two-layer baroclinic ocean to a stationary, axially-symmetric hurricane. *J. Atmos. Sci.*, **24**, 208-215.
- O'Brien, J. and H. Hurlburt, 1972. A numerical model of coastal upwelling. *J. Phys. Oceanogr.*, **2**, 14-26.
- O'Brien, J., 1986. Advanced physical oceanographic numerical modelling. D. Reidel Publishing Company, Dordrecht, 608 pp.
- Omstedt, A., 1989. Matematiska modeller för Östersjön, Skagerrak och Nordsjön. *SMHI FoU-Notiser, R&D Notes*, No. **61**, Norrköping, 44 pp.
- Palmén, E., 1930. Untersuchungen über die Strömungen in den Finnland umgebenden Meeren, *Soc. Sc. Fenn., Comm. Phys.-Math*, V.12. Helsinki, 27 pp.
- Sarkkula, J. and M. Virtanen, 1978. Modelling of water exchange in an estuary. *Nordic Hydrology*, **9**, 43-56.
- Sarkkula, J., 1989. Measuring and modelling flow and water quality in Finland. *Vituki Monographies*, **49**. Water Resources Centre, Budapest, 39 pp.
- Simons, T.J., 1974. Verification of numerical models of Lake Ontario. Part I: Circulation in spring and early summer. *J. Phys. Oceanogr.*, **4**.

- Simons, T.J., 1976. Topographic and baroclinic circulations in the southwest Baltic. *Berichte aus dem Institute für Meereskunde an der Universität Kiel*, No. **25**, Kiel.
- Simons, T.J., 1978. Wind-driven circulations in the southwest Baltic. *Tellus*, **30**, 272-283.
- Svansson, A., 1976. The Baltic circulation. A review in relation to ICES/SCOR Tas.3. *Proceedings of the 10h Conference of the Baltic Oceanographers*, Göteborg, Sweden, paper No. **11**, 10 pp.
- Tamsalu, R., 1967. Calculation of the vertically mean currents in the Tallinn Bay. In: *Marine gulfs as waste water reservoirs* (Kaleis, M. ed.). Zvaige, Riga, 201 pp (in Russian).
- Tamsalu R. and K. Myrberg, 1995. Ecosystem modelling in the Gulf of Finland. Part 1. General features and hydrodynamic prognostic model FINEST. *Estuarine, Coastal and Shelf Science*, **41**, 249-273.
- Tamsalu, R. and P. Ennet, 1995. Ecosystem modelling in the Gulf of Finland. Part 2. The aquatic ecosystem model FINEST. *Estuarine, Coastal and Shelf Science*, **41**, 429-458.
- Tamsalu, R. (ed.) 1996. Coupled 3D hydrodynamic and ecosystem model FINEST. *EMI Report Series*, No. **5**, Tallinn.
- Uusitalo, S., 1960. The numerical calculation of wind effect on sea level elevations. *Tellus* **12**, 427-435.
- Voltzinger, N. and L. Simuni, 1963. Numerical integration of the shallow sea equations and the Leningrad storm surge forecasting. *Proceedings, Gosudarstvennoy Okeanograficeskii Institut*, **74**, 33-44 (in Russian).
- Welander, P., 1966. A two-layer frictional model of wind-driven motion in a rectangular oceanic basin. *Tellus*, **18**, 54-62.
- Welander, P., 1968. Wind-driven circulation in one-and two-layer oceans of variable depth. *Tellus*, **29**, 1-16.
- Witting, R., 1910. Suomen Kartasto. - Karttalehdet nr. 6b, 7,8 ja 9. Rannikkomeret (Atlas de Finlande. - Cartes N:os 6b, 7,8,9. Mers environnates). Finnish Institute of Marine Research, Helsinki.
- Witting, R., 1912. Zusammenfassende Übersicht der Hydrographie des Bottnischen und Finnischen Meerbusens und der Nördlichen Ostsee. *Finnlands Hydrographis-Biologische Untersuchungen*, No.7.
- Zilitinkevich, S.S. (ed.), 1991. *Modelling Air-Lake Interaction*. Springer-Verlag, Heidelberg, 129 pp.

This paper was not presented in the seminar, it is included here since the results are closely related to the topics of the other presentations.

Fig. 1. The time evolution of wind speed in m/s (A) and wind stress (B) in m^2 / s^2 during August 1-31, 1992 at the Kalbådagrund weather station in the Gulf of Finland. The measured wind speeds and wind stresses at Kalbådagrund are marked with continuous lines, the interpolated HIRLAM parameters with dash-dotted lines, and the corrected (by Eq. 20) interpolated HIRLAM parameters with dashed lines.

Fig. 2. Surface salinity fields in the Gulf of Finland. (A): simulated by the 2DK model version using the atmospheric forcing derived from the Kalbådagrund weather station and (B): simulated by the 2DH model version using the atmospheric forcing from HIRLAM. The figures represent the mean of model results from August 18-21. Positions of the salinity measurements carried out between August 18-21 are marked with a black dot (according to model results changes in the horizontal salinity field were small during August 18-21). The isoline analysis of the model results is shown at intervals of 0.2 PSU.

Fig. 3. Surface temperature field in the Gulf of Finland. (A): simulated by the 2DK model version using the atmospheric forcing derived from the Kalbådagrund weather station and (B): simulated by the 2DH model version using the atmospheric forcing from HIRLAM. The figures represent the situation on August 20 at 12 GMT. Observed values are marked by a black dot with the corresponding value. The isoline analysis of the model results is shown at intervals of 0.1 degrees (A) and of 0.2 degrees (B).

Fig. 4. Time evolution of temperature in the upper mixed layer at station GR6 (59 deg. 41 min.N, 23 deg. 34 min.E). The continuous line represents results as simulated by the 2DH model, the broken line those of the 2DK model.

Fig. 5. Fields of the thickness of the upper mixed layer in the Gulf of Finland simulated by the 2DH model version. The figures represent the situation at 12 GMT each day: August 18 (A), August 20 (B). Observed values are shown by a black dot with the corresponding value. The isoline analysis of the model results is shown at intervals of 2 metres.

Fig. 6. Currents in the upper mixed layer of the Gulf of Finland. The figures represent the situation on August 27 at 12 GMT. (A): as simulated by the 2DK model, (B): as simulated by the 2DH model.

Fig. 7. Time evolution of water level height at the coastal station of Hamina (60 deg., 35 min.N, 27 deg., 10 min.E) in the Gulf of Finland on August 1-31, 1992. The measured water level is marked with a continuous line, the 2DK model results with + symbol and the 2DH model results with a broken line.